의학박사학위논문

Synthesis of targeted ultrasound contrast agent containing chemotherapeutic drug and *in vitro* evaluation in HER2-positive gastric cancer cell line

항암제 함유 표적 초음파조영제의 합성 및 HER2-양성 위암세포주를 대상으로 한 시험관내 효과분석에 대한 연구

2016년 2월

서울대학교 대학원

임상의과학과

이 윤 진

의학박사학위논문

Synthesis of targeted ultrasound contrast agent containing chemotherapeutic drug and *in vitro* evaluation in HER2-positive gastric cancer cell line

항암제 함유 표적 초음파조영제의 합성 및 HER2-양성 위암세포주를 대상으로 한 시험관내 효과분석에 대한 연구

2016년 2월

서울대학교 대학원

임상의과학과

이 윤 진

A thesis of the Degree of Doctor of Philosophy

항암제 함유 표적 초음파조영제의 합성 및 HER2-양성 위암세포주를 대상으로 한 시험관내 효과분석에 대한 연구

Synthesis of targeted ultrasound contrast agent containing chemotherapeutic drug and *in vitro* evaluation in HER2-positive gastric cancer cell line

February 2016

The Department of Clinical Medical Sciences,
Seoul National University
College of Medicine
Yoon Jin Lee

Synthesis of targeted ultrasound contrast agent containing chemotherapeutic drug and *in vitro* evaluation in HER2-positive gastric cancer cell line

지도 교수 이 학 종

이 논문을 의학박사 학위논문으로 제출함

2015년 10월

서울대학교 대학원
임상의과학과
이 윤 진

이윤진의 의학박사 학위논문을 인준함

2015년 12월

위 원 장 _____ (인)

부위원장 _____ (인)

위 원 _____ (인)

위 원 _____ (인)

위 원 _____ (인)

Synthesis of targeted ultrasound contrast agent containing chemotherapeutic drug and *in vitro* evaluation in HER2-positive gastric cancer cell line

by
Yoon Jin Lee

A thesis submitted to the Department of Clinical Medical Sciences in partial fulfillment of the requirements for the Degree of Doctor of Philosophy in Clinical Medical Sciences at Seoul National University College of Medicine

December 2015

Approved by Thesis Committee:

Professor _____ **Chairman**

Professor _____ **Vice chairman**

Professor _____

Professor _____

Professor _____

ABSTRACT

Synthesis of targeted ultrasound contrast agent containing chemotherapeutic drug and *in vitro* evaluation in HER2-positive gastric cancer cell line

Yoon Jin Lee

Department of Clinical Medical Sciences

College of Medicine, Seoul National University

Introduction: Gastric cancer is one of the leading causes of cancer mortality. HER-2 is a well-established molecular target for treatment of advanced gastric cancer. For effective targeted delivery chemotherapeutic drug to HER2-positive gastric cancer, we aimed to synthesize and evaluate an ultrasound contrast agent conjugated with trastuzumab for targeted delivery of chemotherapeutic drug to HER2-positive gastric cancer *in vitro*.

Materials and Methods: Experiments involving animals were approved by the

Institutional Animal Care and Use Committee. Human gastric cancer cell lines NCI-N87, SNU-216, SNU-484 and SNU-601 were obtained and incubated. We synthesized a HER2-targeted microbubble contrast material by forming a microbubble liposome complex (MLC) from mixing lipids and sulfur hexafluoride gas core. The MLC was conjugated with anti-HER2 antibody (trastuzumab, Herceptin®) to target Her2-positive gastric cancer cells. The MLC-$HER2_{Ab}$ was fluorescent-labeled, incubated with gastric cancer cells, and then evaluated under confocal laser scanning microscopy for cellular targeting. Next, cisplatin was conjugated with the MLC-$HER2_{Ab}$, and incubated with NCI-N87 and SNU-484 gastric cancer cells to assess the cytotoxicity induced by the therapeutic agent. Ultrasound exposure was additionally performed to investigate the effect of ultrasound-mediated delivery of the complex.

Results: Under confocal microscopy, highly selective cell targeting for HER2-positive cell lines NCI-N87 and SNU-216 was observed. In NCI-N87 cells, cisplatin conjugated MLC-$HER2_{Ab}$ showed increase in cell death after the exposure of ultrasound. This effect was not observed in SNU-484 cells.

Conclusions: Microbubble liposome complex can specifically target HER2-positive gastric cancer cell lines by the conjugation of trastuzumab. It can also readily deliver cisplatin to target cells under ultrasound, resulting in effective cancer cell death. Therefore, MLC may provide a promising method for ultrasound-mediated targeted drug delivery.

Keywords: ultrasound, microbubble, targeted therapy, gastric cancer

Student Number: 2013 – 30827

CONTENTS

LIST OF TABLES AND FIGURES

LIST OF ABBREVIATIONS

MB – microbubble

Lipo – liposome

MLC – microbubble liposome complex

HER2 – human epidermal growth factor receptor type 2

US – ultrasound

FITC – fluorescein isothiocynate

CLSM – confocal laser scanning microscopy

Cis – cisplatin

INTRODUCTION

Gastric cancer is the fifth most common cancer (6.8% of the total) and the third leading cause of cancer death (8.8% of the total) worldwide (1). According to GLOBOSCAN 2012, most cases (more than 70%) occur in developing countries, and half the world total occurs in Eastern Asia with higher mortality rates (1). In Korea, gastric cancer is the second most common cancer and the third leading cause of cancer mortality (2). Curative treatment of gastric cancer can only be achieved by radical gastrectomy. However tumor recurrence is common, being detected in approximately 60% of patients (3). Moreover, gastric cancer is often diagnosed at an advanced stage, where systemic chemotherapy is the mainstay of treatment (4, 5).

For patients in advanced stage, 5-fluorouracil with plus platinum agents are widely accepted regimens of standard treatment (5). This chemotherapeutic regimen offers a response rate of 30%-50% with a median overall survival of 9 to 11 months (6). Because of the poor survival outcomes of conventional chemotherapeutic agents, attention has turned to potential molecular targets in gastric cancer in keeping with the recent trends of tailored medicine.

The human epidermal growth factor receptor (EGFR) family, which is one of the most popular targets in human cancer therapy, includes four members, HER1 (ErbB1, also known as EGFR), HER2 (ErbB2), HER3 (ErbB3) and HER4 (ErbB4) (7). Among them, human epidermal receptor 2 (HER2) is overexpressed in 10-20% of gastric cancer patients and is known to be associated with poor prognosis and distant metastasis (8-10). Trastuzumab, a recombinant humanized monoclonal antibody targeting the extracellular domain IV of the HER2 protein, has been shown to improve radiological response rate, progression-free survival and overall survival when added to cisplatin and fluoropyrimidine chemotherapy for advanced

gastric cancer patients in a phase III clinical trial, known as the ToGA trial (11).

Microbubbles have been used as contrast agents for ultrasound imaging, but are recently being explored for therapeutic purposes (12). They were initially studied for anti-angiogenic therapy (13, 14). However, there is increasing interest in investigating the targeted or enhanced delivery effects of microbubbles both in detection (15, 16) and therapy (17, 18) of diseases.

Therefore, we aimed to enhance the delivery of cisplatin into HER2-positive gastric cancer cells by using microbubble contrast agents designed for ultrasound. We developed a "microbubble liposome complex (MLC)", carrying cisplatin with antibody targeting HER2 in order to improve specific delivery into target cells. The main purpose of this study was to evaluate the efficacy of cellular targeting and delivery of chemotherapeutic drug by using microbubble with therapeutic ultrasound, and to explore the feasibility of clinical applications of ultrasound-guided therapy for advanced gastric cancer using targeted MLC.

MATERIALS AND METHODS

1. Cell lines and culture

Experiments involving animals were approved by the Institutional Animal Care and Use Committee. Human gastric cancer cell lines NCI-N87, SNU-216, SNU-484, SNU-601 were supplied by Korean Cell Line Bank (19). N87 and SNU216 are cell lines in which HER2 gene amplification has been shown (20, 21). Cells were cultured in RPMI-1640 media supplemented with 10% fetal bovine serum and 1% penicillin-streptomycin, and were maintained at 37 ºC in a humidified atmosphere containing 5% CO_2. Cells were harvested from subcultures at confluence, and washed, trypsinzed with 0.01% trypsine EDTA (Sigma-Aldrich, St. Louis, MO, USA), and re-suspended in fresh culture media for experiments.

2. Chemotherapeutic drug

Cisplatin with molecular weight of 300.01 g/mol was purchased from JW Pharmaceutical Korea Ltd.

3. Preparation of microbubble liposome complex

To prepare the microbubble (MB), lipid stocks of 15.4 mg of DPPC (1,2-dipalmitory-sn-glycero-3-phosphatidylcholine, Avanti, Alabaster, AL, USA), 3.5

mg of cholesterol, 1.0 mg of DCP (dicetyl phosphate, Avanti), 1.2 mg of DPPE (1,2-dipalmitory-sn-glycero-3-phosphoethanolamine, Sigma-Aldrich) and 5.0mg of DSPE-PEG-SPDP (1,2-distearoyl-sn-glycero-3-phosphoethanolamine-N-[PDP(polyethylene glycol)-2000], Avanti) were dissolved into 5.0 mL of chloroform (99.9%, Sigma-Aldrich). For removal of the solvent, the lipid mixture was evaporated for 5 min at 35 °C and freeze-dried for 24 hours at -45 °C, which created the phospholipid film. To make a lipid solution, a 2-mL mixture of glycerin, propylene, and H_2O at a volume ratio of 1:2:7 was added to the film and transferred to a hermetic vial (Wheaton, Millville, NJ, USA). After filling the vial with sulfur hexafluoride (SF_6) gas, mechanical mixing with a high-speed shaking-device (KIMS, South Korea) led to the formation of microbubbles.

To create liposomes (Lipo), a lipid mixture was made in a similar manner. DPPC (15.4mg), DCP (1.0mg), DPPE (1.2mg) and cholesterol (3.5mg) were mixed in 5.0 mL of chloroform. A lipid film was produced after evaporating for 5 minutes at 35 °C and lyophilizing for 24 hours at -45 °C. Two milliliters of H_2O was added to the film, and the mixture was agitated by a sonicator (Sigma Aldrich) for 5 minutes at 60 ºC. The film solution underwent 5 cycles of freezing in liquid nitrogen and defrosting in a water bath. In order to make a large unilamellar vesicle, the liposomal dispersion was extruded through a mini-extruder (Avanti) containing a polycarbonate filter with a pore size of 200 nm at 60 ºC. For the addition of sulfhydryl functional group on the surface of the liposome, amine-active liposome, derived from DPPE, was treated with 5 mg 2-iminothiolane·HCl (Traut's reagent, Pierce) for 2 hours at 25 °C after adjusting the pH to 8 with 1 M $NaHCO_3$.

To produce the microbubble liposome complex (MLC), 0.67 mL of thiol-active microbubbles (13mg/mL, 1.2 x 10^{11} microbubbles/mL), derived from DSPE-PEG-PDP, were mechanically shaken together with 2mL of thiolated liposomes (10mg/mL) at room temperature for 2 hours in a dental amalgamator. The MLC solution with an amine functional group was treated with 5 mg of sulfosuccinimidyl-4-(N-maleimidomethyl)cyclohexane-1-carboxylate (sulfo-SMCC, Sigma Aldrich) for 3 hours at 25°C after adjusting the pH to 8.2 with 1 M $NaHCO_3$ in order to active the maleimide functional group. Afterwards, this solution was conjugated with half antibody of anti-human epidermal growth factor receptor type 2 (HER2) monoclonal antibodies (Trastuzumab, Herceptin®, Roche, Basel, Switzerland) by additional mechanical shaking at 4 ℃ for 24 hours to target HER2 expressed in gastric cancer cell lines (20, 21).

4. Characterization of MLC particles

For characterization of the synthesized MLC particles, optical micrograph images were obtained. In particular, fluorescent microbubbles with fluorescein isothiocyanate (FITC, Sigma Aldrich) were used for enhanced visualization. The sizes of MLC particles were measured by the dynamic light scattering analysis method. The loading efficiency of trastuzumab on the liposome was measured by ultraviolet-visible (UV-Vis) spectroscopy (Scinco, Seoul, Korea). The standard curve of ultraviolet absorbance for trastuzumab was obtained. After loading, the mixture was washed to remove the unloaded trastuzumab from MLC-$HER2_{Ab}$ by centrifugation at 13000 rpm for 5 minutes. Then, the concentration of trastuzumab

in the supernatant was measured by UV-Vis spectroscopy. The loading efficiency was calculated as follows: (concentration of trastuzumab before loading – concentration of trastuzumab in the supernatant after loading) / (concentration of trastuzumab before loading) x 100%.

5. Analysis of cellular targeting effect

To make fluorescent MLCs, FITC (1mg, Sigma Aldrich) was added to the lipid solution before the mixing step during microbubble synthesis. Hydrophilic organic dye (Texas red, 1mg, Sigma Aldrich) was added to the film solution during the liposome synthesis. Accordingly, fluorescence-labelled MLCs were made which emitted green fluorescence from the microbubbles and red fluorescence from the liposomes. NCI-N87, SNU-216, SNU-484 and SNU-601 cells were seeded in 1 well and 4 well chamber slides (SPL, Pocheon, Korea) at a density of 1 x 10^5 cells per well. Then, three types of solutions (control media, MB-FITC-Lipo-Texas red, MB-FITC-Lipo-Texas red-$HER2_{Ab}$) were applied to the cells and they were incubated for 3 hours at 37 ºC in 5% CO_2.

After washing the cells with cold phosphate buffered saline for removal of unattached MLCs, the cells in 1 well chamber slides containing MB-FITC-Lipo-Texas red-$HER2_{Ab}$ were exposed to ultrasound using an ultrasound scanner (iU22, Philips Ultrasound) equipped with a 5-12 MHz broadband linear array transducer with 256 elements in a diameter of 3.5 cm. The cells were seeded in a line in the chamber slide and submerged in buffered saline. Subsequently, the cells were treated with ultrasound with a bandwidth ranging from 5 to 12 MHz and a center

frequency of 9 MHz at intervals of 3 seconds for 3 minutes. The mechanical index was set at 0.61. This procedure was named “US-flashing”.

The treated cells were additionally incubated for 3 hours at 37 ºC. To identify the targeting effect of MLC, a confocal laser scanning microscopy (CLSM) was used (Leica, Wetzlar, Germany). The fluorescence emission from FITC (excitation, 488 nm; emission, 500-570 nm) and Texas red (excitation, 594nm; emission, 600-680 nm) were analyzed. The fluorescence intensities of the cells were analyzed quantitatively (Leica Application Suite Advanced Fluorescence Lite). The experiments were done in triplicates under the same conditions. Differential interference contrast (DIC) and 4’6-diamidino-2-phenylindole (DAPI) for nuclear staining images were also obtained.

6. Cisplatin loading into MLC

Another type of MLC was made by conjugation with cisplatin for enhanced chemotherapeutic effect. To produce this complex (MLC-$HER2_{Ab}$-Cis), 1 mg of cisplatin was added to MLCs and dissolved in 2 mL of H_2O. The mixture was agitated by a sonicator, underwent freezing and defrosting, and was filtered using 200 nm-sized polycarbonate filters as previously described.

The loading efficiency of cisplatin in the liposome was measured by ultraviolet-visible (UV-Vis) spectroscopy (Scinco, Seoul, Korea). The standard curve of ultraviolet absorbance for cisplatin was obtained. The ultraviolet detection was maximal at 297.89 nm. After loading, the mixture was washed to remove the unloaded cisplatin from MLC-$HER2_{Ab}$-Cis by centrifugation at 13000 rpm for 5

minutes. Then, the concentration of cisplatin in the supernatant was measured by UV-Vis spectroscopy. The loading efficiency was calculated as follows: (concentration of cisplatin before loading – concentration of cisplatin in the supernatant after loading) / (concentration of cisplatin before loading) x 100%.

7. Cell viability assay according to MLC delivery and US-flashing

NCI-N87 and SNU-484 cells were seeded at a concentration of 4.0 x 10^3 cells, and 3.0 x 10^3 cells per well, respectively in a 96-well tissue culture plate. After an overnight incubation at 37 ºC under 5% CO_2, the cells were treated with five different methods as follows: (a) no treatment (group 1, control), (b) MLC-$HER2_{Ab}$ without US-flashing (group 2), (c) MLC-$HER2_{Ab}$ with US-flashing (group 3), (d) MLC-$HER2_{Ab}$-Cis without US-flashing (group 4), and (e) MLC-$HER2_{Ab}$-Cis with US-flashing (group 5). The MLC-$HER2_{Ab}$-Cis solutions were added at different concentrations of cisplatin (6.3 μM, 12.5 μM, 25 μM, 50 μM) into the culture media and the cells were allowed to grow for 3 hours. Then, the cells were washed to remove the unattached MLCs. The cells in group 3 and 5 underwent US-flashing as described above in section 5. Light microscopic images were obtained for the five groups just before cell viability assay.

Next, cell viability was assessed using the EZ-CyTox cell viability assay kit (Daeil Lab Service, Seoul, Korea) based on the 4-[3-(4-iodophenyl)-2-(4-nitrophenyl)-2H-5-tetrazolio]-1,3-benzene disulfonate (WST-1) assay method (22), immediately (3 hours after initial incubation) and after 72 hours of incubation (75

hours after initial incubation). EZ-CyTox reagent of 10 μL was added to each well and incubated for an additional 4 hours at 37 ºC. The absorbance was measured at 450 nm in a spectrophotometer (Scinco). The percentage of viable cells was calculated as follows: (absorbance of experimental well / absorbance of control well) x 100%. The measurements were performed in triplicates under the equivalent conditions.

8. Statistical analysis

Data were expressed as means and standard errors for triplicate measurements. One-way analysis of variance (ANOVA) was performed to evaluate the differences of cell viabilities in each group. Tukey's multiple comparison test was used for comparison between each groups. Statistical analyses were performed using IBM SPSS Statistics for Windows software, version 22.0 (IBM Corp., Armonk, NY, USA). A P value less than 0.05 was considered as statistically significant.

RESULTS

1. Character of synthesized MLC particles

The sizes of finally synthesized microbubbles, MLC and MLC-$HER2_{Ab}$ measured between 100 and 200 nm with an average size of 150nm. Figure 1 shows the optical micrograph of MLC particles.

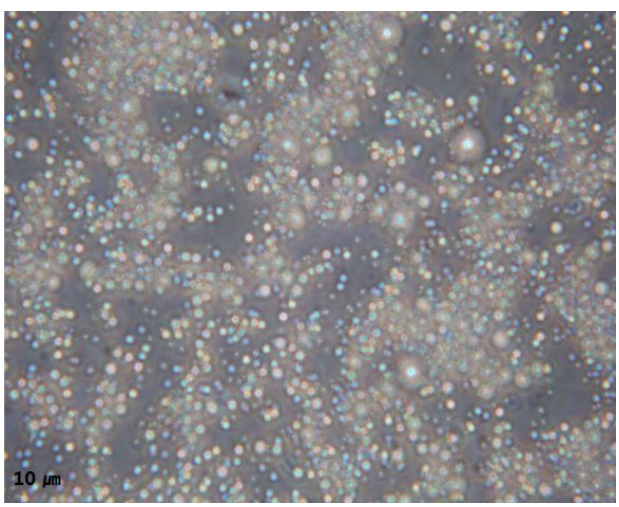

Figure 1. Optical micrograph images MLC particles. Scale bar, 10 ㎛.

The loading efficiency of trastuzumab was 37.8%. The concentration of trastuzumab before loading was 17.2 μM. The concentration of loaded trastuzumab

in the MLC-$HER2_{Ab}$ was 6.5 μM.

2. Cellular targeting effect of MLC

The MLC-$HER2_{Ab}$ was shown to be able to target HER2-positive NCI-N87 and SNU-216 cells. CLSM images showed green fluorescence indicating labeled microbubbles and red fluorescence indicating labeled liposomes in NCI-N87 cells (Figure 2-1) and SNU-216 cells (Figure 2-2), both before and after US-flashing.

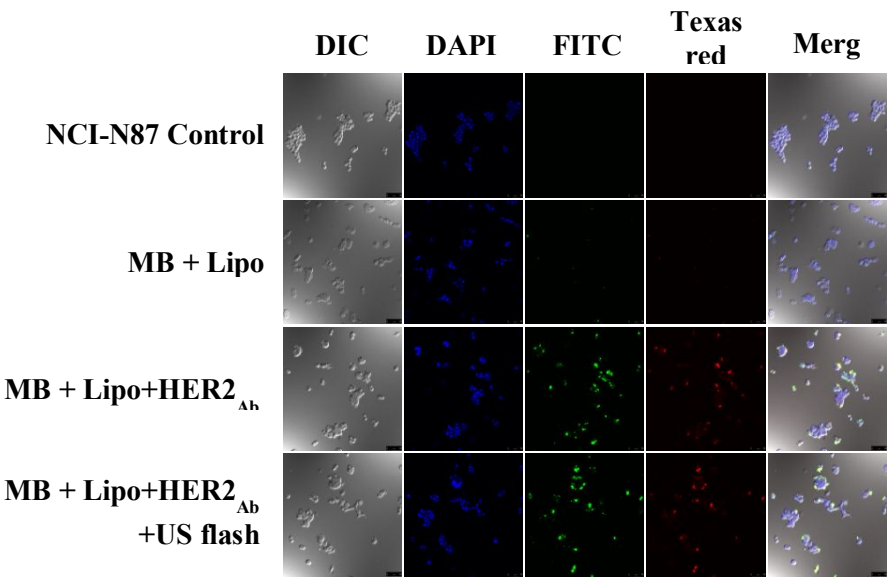

Figure 2-1. Confocal laser scanning microscopy images of NCI-N87 cells. Green fluorescent cells labeled by FITC and red fluorescent cells labeled by Texas red are observed before and after ultrasound-flashing.

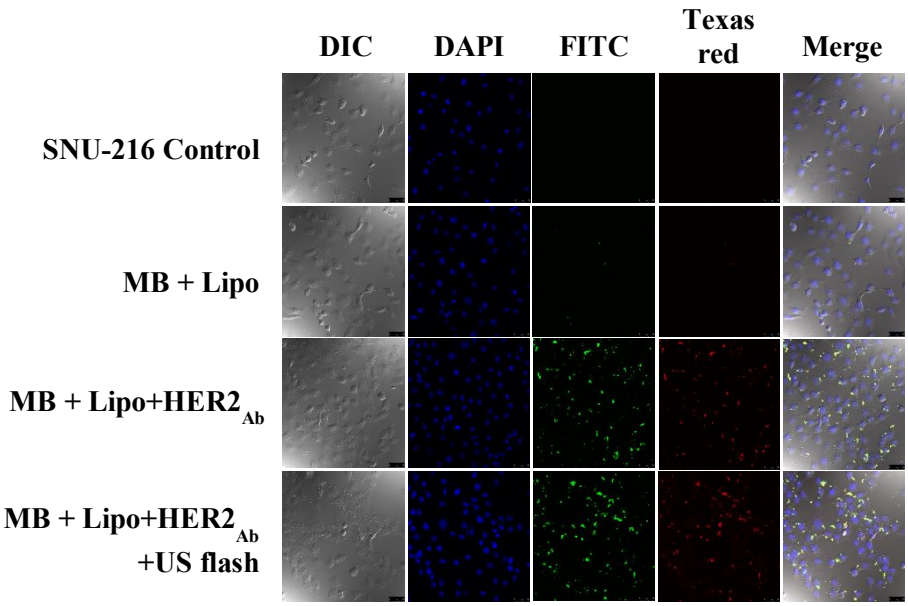

Figure 2-2. Confocal laser scanning microscopy images of SNU-216 cells. There are green fluorescent cells labeled by FITC and red fluorescent cells labeled by Texas red before and after ultrasound-flashing.

On the other hand, no additional green or red fluorescent cell were seen on CLSM images of SNU-484 cells (Figure 2-3) and SNU-601 cells (Figure 2-4), before and after US-flashing, compared with the control images before the incubation with MLCs. This suggests poor targeting of HER2-negative cells by MLC-$HER2_{Ab}$.

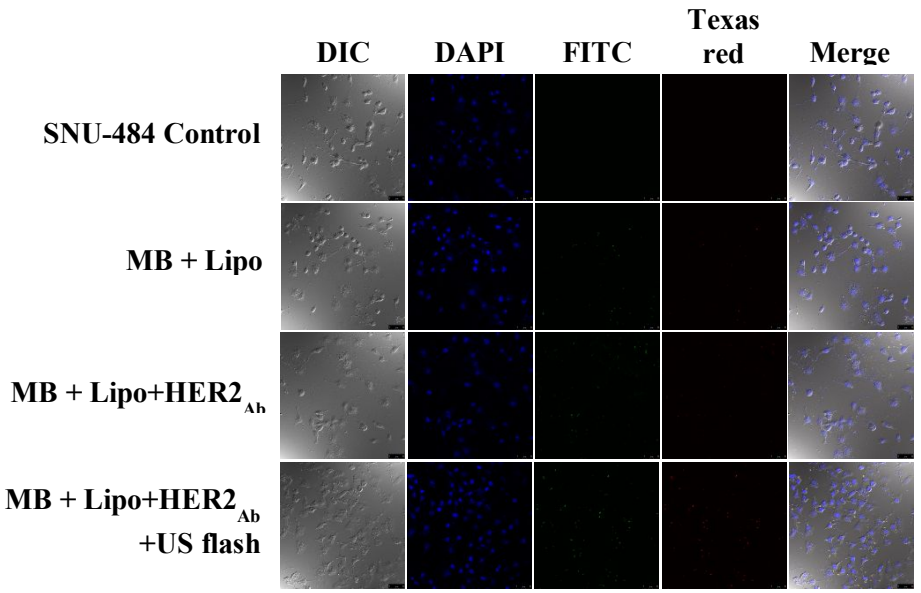

Figure 2-3. Confocal laser scanning microscopy images of SNU-484 cells. There are no visible green or red fluorescent cells under microscopy suggesting poor cellular targeting of MLC-$HER2_{Ab}$.

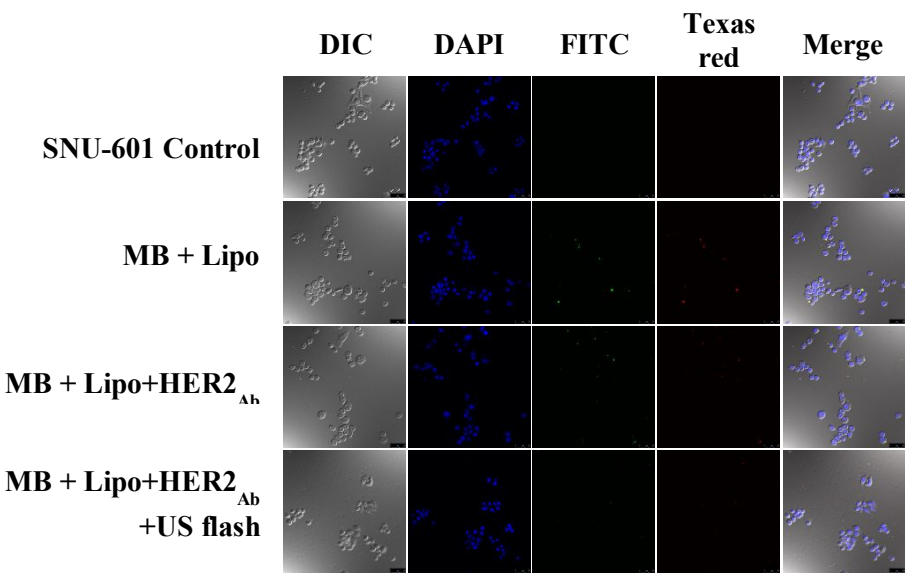

Figure 2-4. Confocal laser scanning microscopy images of SNU-601 cells. No

green or red fluorescent cells are seen under microscopy suggesting poor cellular targeting of MLC-HER2$_{Ab}$.

Figure 2-5 shows the fluorescence intensities of the delivered MLCs on confocal microscopy before and after US-flashing in NCI-N87, SNU-216, SNU-484, SNU-601 cells, respectively. There are stronger fluorescence intensities both for FITC (Figure 2-5A) and Texas red (Figure 2-5B) in HER2-positive NCI-N87 and SNU-216 cells than in HER2-negative SNU-484 and SNU-601 cells, in the presence of MLC-HER2$_{Ab}$, before and after ultrasound exposure. These bar graphs represent the selective targeting ability of MLC-HER2$_{Ab}$ depending on the HER2 expression status, which are equal or stronger after US-flashing.

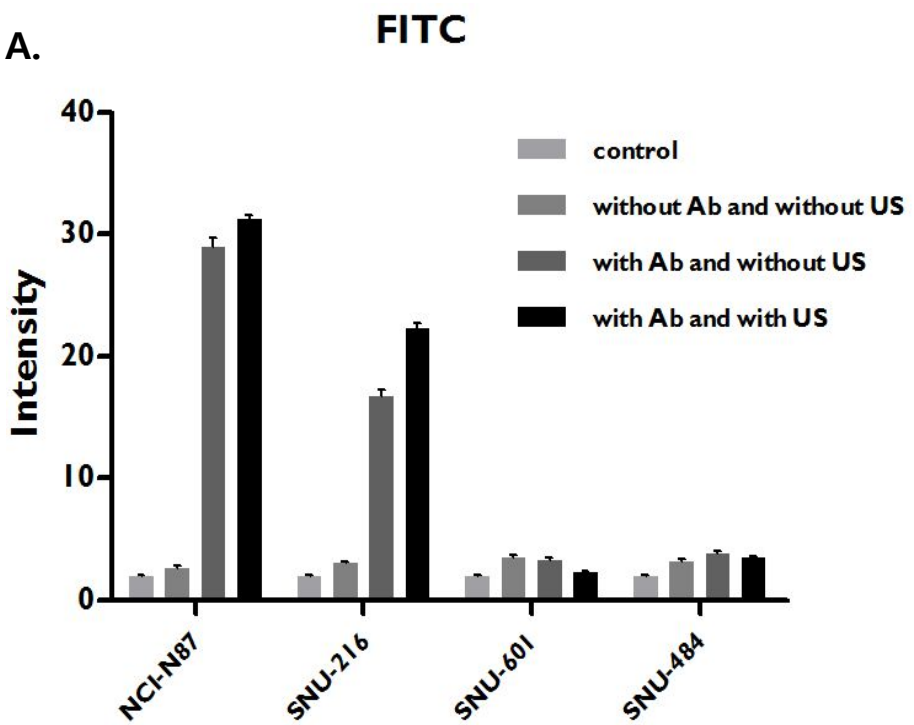

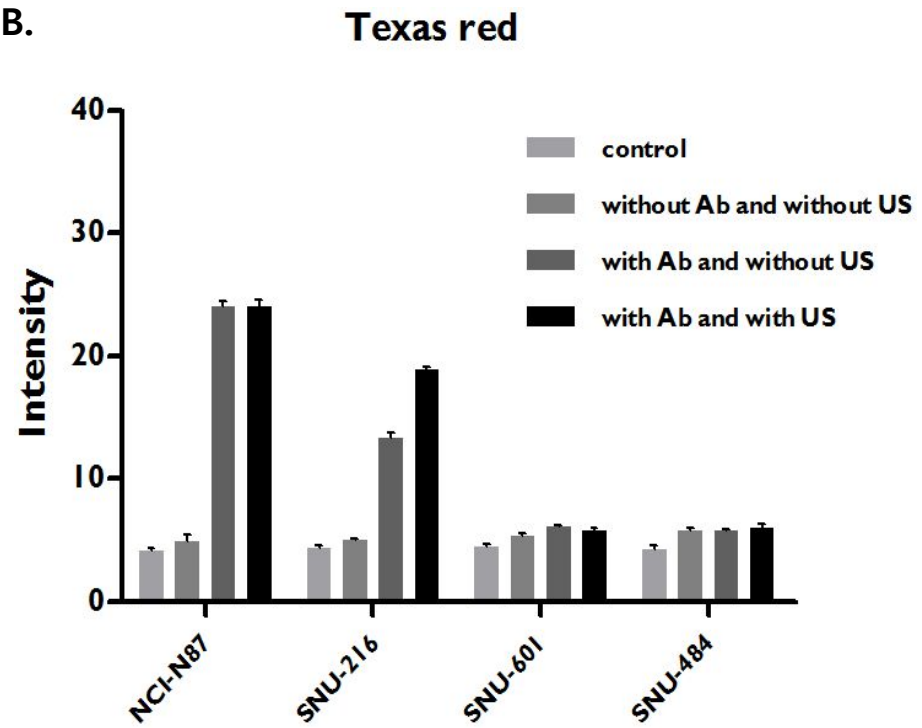

Figure 2-5. Bar graphs depicting signal intensity of fluorescence according to cell lines (A: FITC, B: Texas red). The fluorescence intensities of HER2-positive NCI-N87 and SNU-216 cells are higher than in HER2-negative SNU-484 and SNU-601 cells, in the presence of MLC-$HER2_{Ab}$ before and after ultrasound exposure.

3. Efficiency of cisplatin loading into MLC

The efficiency of cisplatin loading into MLC-$HER2_{Ab}$ was 58.54%. The concentration of cisplatin before loading was 1.7 μM. The concentration of loaded cisplatin in the MLC-$HER2_{Ab}$ was 1 μM. Figure 3 shows the signal intensity curve of ultraviolet absorption before and after loading of cisplatin according to wavelength.

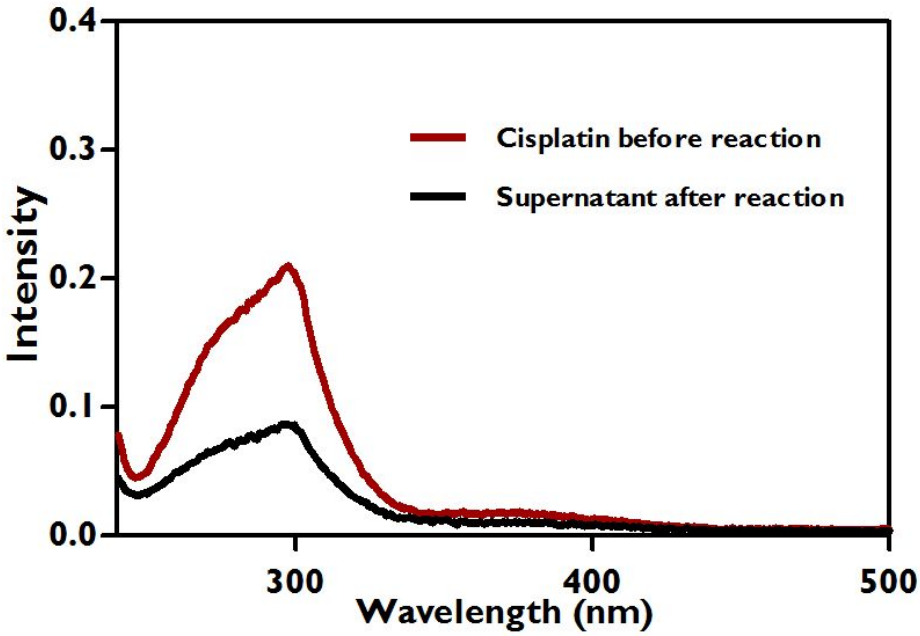

Figure 3. Loading efficiency of cisplatin into MLC. The curve presents the difference of ultraviolet absorptions before and after the loading of cisplatin. The loading efficiency measured to be 58.54%.

4. Cellular viability after MLC delivery and US-flashing

The MLC with cisplatin concentration of 50 μM was chosen for analysis. In NCI-N87 cells (Figure 4-1 and 4-2), the cell viability rate at 3 hours was also more than 80% in all three groups with significantly decreased viability of group 4 (MLC-$HER2_{Ab}$-Cis without US-flashing, 81.53 ± 5.335 %) compared to group 1 (control) (P = 0.0004). The cellular viability of group 4 was also significantly lower than group 2 (MLC-$HER2_{Ab}$ without US-flashing, 92.13 ± 9.706 %) (P = 0.0295). After 75 hours of incubation, group 4 (MLC-$HER2_{Ab}$-Cis without US-flashing, 91.61 ± 9.824 %) and group 5 (MLC-$HER2_{Ab}$-Cis with US-flashing, 83.47 ± 5.112 %)

showed a tendency to decrease in cell viability rate compared to group 1 (control) without statistical significance (P = 0.7351 and 0.1426, respectively). When the cellular viabilities were compared to evaluate the effect of US-flashing, the viability values were slightly lower without statistical significance in group 3 compared to group 2 (121.5 ± 23.36 % vs. 125.4 ± 5.552 %, P = 0.9779), and in group 5 compared to group 4 (83.47 ± 5.112 % vs. 91.61 ± 9.824 %, P = 0.7556). However, the viability values were significantly lower in group 4 compared to group 2 (91.61 ± 9.824 % vs. 125.4 ± 5.552 %, P = 0.0004) and in group 5 compared to group 3 (83.47 ± 5.112 % vs. 121.5 ± 23.36 %, P < 0.0001), indicating significant cytotoxic effect of additional cisplatin resulting in the lowest cellular viability in group 5 (MLC-$HER2_{Ab}$-Cis with US-flashing, 83.47 ± 5.112 %).

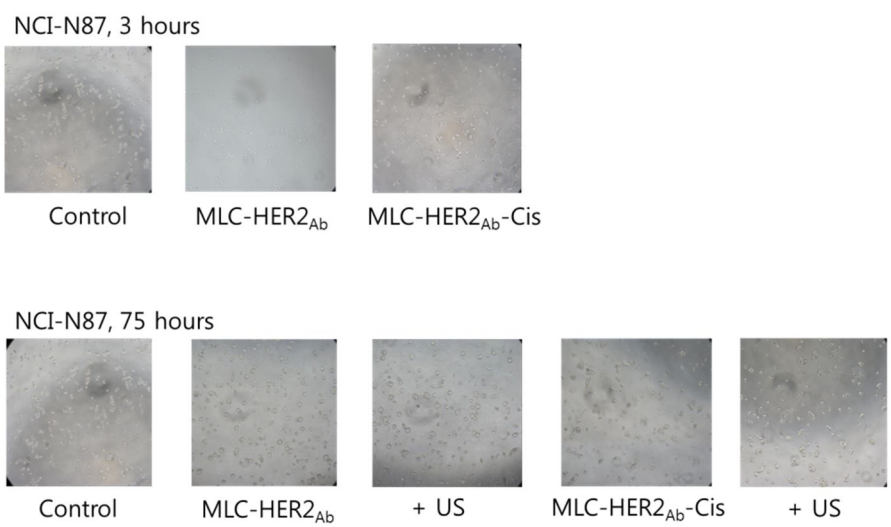

Figure 4-1. Light microscopic images of NCI-N87 cells at 3 hours and 75 hours after incubation. Decreased cell viability of group 4 and group 5 can be seen at 75 hours.

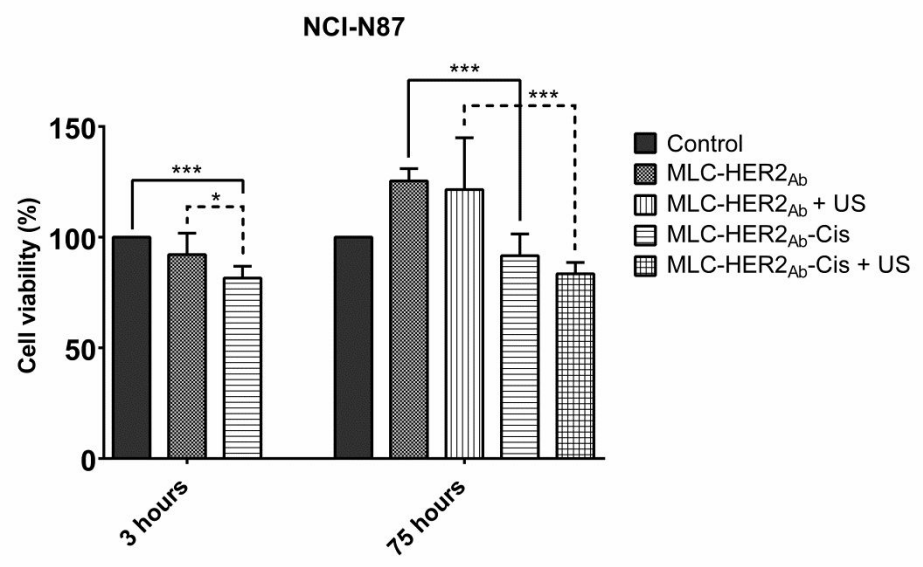

Figure 4-2. Bar graph depicting cell viability assay results of NCI-N87 cells at 3 hours and 75 hours after incubation. Decreased viability of NCI-N87 cells treated with MLC-$HER2_{Ab}$-Cis with and without US-flashing is noted. ***P < 0.001, *P < 0.05

In SNU-484 cells (Figure 4-3 and 4-4), there was no significant difference in cell viability among the 3 groups) at 3 hours (range 95.53% ~ 101.1%, P = 0.5284). After 75 hours of incubation, the cell viability rates were above 100% without significant difference among the five groups (range 103.9% ~ 106.1%, P = 0.7094). Addition of cisplatin into the MLC did not show cytotoxic effect. US-flashing also did not increase the extent of cell death.

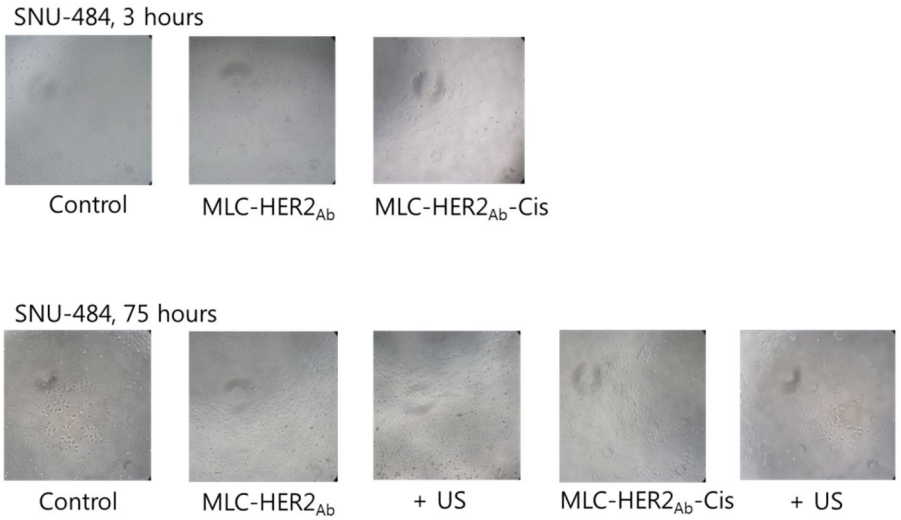

Figure 4-3. Light microscopic images of SNU-484 cells at 3 hours and 75 hours after incubation. There is no significant difference in cell viability among the control and experimental groups.

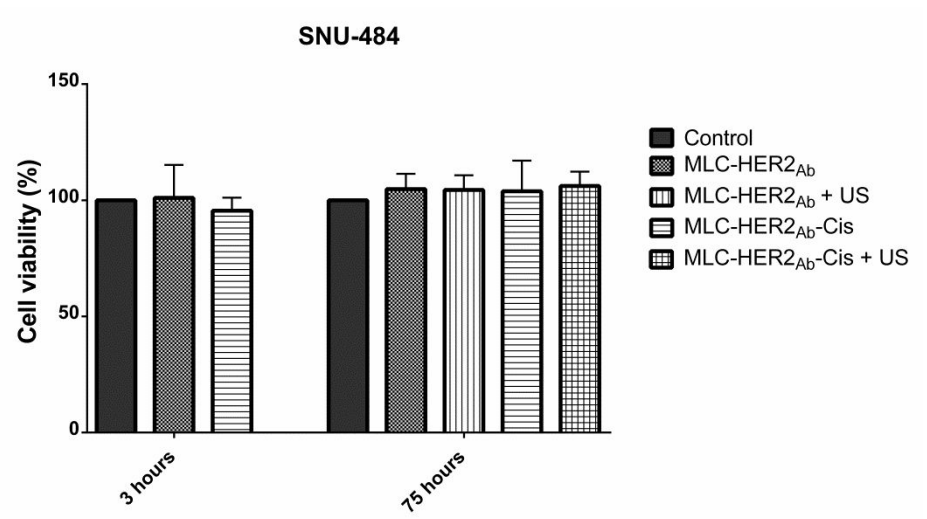

Figure 4-4. Bar graph depicting cell viability assay results of SNU-484 cells at

3 hours and 75 hours after incubation. There is no significant difference in cell viability among the three groups at 3 hours and among the five groups at 75 hours.

DISCUSSION

In this study, we aimed to enhance targeted cellular delivery of chemotherapeutic agent by using microbubbles. Microbubbles were originally developed to be a gas-containing contrast agent to improve ultrasound imaging, with a mean diameter of 3 μm (23). However, it has also been shown to be an effective carrier of gene and drug delivery, which can be enhanced by sonoporation phenomenon occurring with the destruction of microbubbles upon exposure to ultrasound (24). Selective targeting of certain tissues or cells can be achieved by adding target-specific ligands such as antibodies (17).

We synthesized MLCs conjugated with anti-HER2 antibody to target gastric cancer cell lines with overexpression of HER2 (20, 21). Confocal microscopic images of fluorescent MLCs showed selective delivery of MLCs to NCI-N87 and SNU-216 cells having higher expression of HER2 than SNU-484 and SNU-601 cells. This represents the selective targeting ability of MLC-$HER2_{Ab}$ depending on the HER2 expression status. Therefore, it is possible for MLCs to effectively target gastric cancer cell lines, guided by target-specific antibodies conjugated to the MLCs.

Cisplatin, a chemotherapeutic drug commonly used for gastric cancer was added into the MLCs in this study. It is worth mentioning that cisplatin was loaded into the liposome component of MLCs, rather than being added directly into the media of cell wells, which may enable focused delivery of chemotherapeutic drugs to the target tissue with less cytotoxic effects to non-targeted tissues in systemic chemotherapy. In NCI-N87 cells, MLC-$HER2_{Ab}$-Cis with US-flashing exhibited the lowest cell viability value of 83.47 ± 5.112 % among the five groups at 75 hours after incubation. As efficient targeting of MLCs to NCI-N87 cells was possible due to anti-HER2 antibodies, this result suggests that cisplatin could be

effectively delivered to gastric cancer cells under ultrasound guidance, and induce cell deaths shown by decreased cellular viability measurements.

However, our results are rather limited in showing the targeted therapeutic effect because it was tested on only one HER2-positive cell line, NCI-N87. It would have been more desirable if significantly decreased cellular viability was also observed in SNU-216, the other HER2-positive cell line, when treated with MLC-$HER2_{Ab}$-Cis. Nonetheless, it is known that SNU-216 cell lines have less overexpression of HER2 compared to NCI-N87 cell lines. Therefore, we can postulate that MLC-$HER2_{Ab}$-Cis may not be as effective for SNU-216 cells as in NCI-N87 cells.

Trastuzumab is considered to have a synergistic growth inhibitory effect with cisplatin by increasing the sensitivity of cells to cisplatin (25). The decreased viability of NCI-N87 cells treated with MLC-$HER2_{Ab}$-Cis with and without US-flashing, compared to groups treated with MLC-$HER2_{Ab}$ may also be a reflection of this synergistic effect to some extent. The reported higher growth inhibitory effects of trastuzumab on NCI-N87 cells than SNU-216 cells (26), suggests that NCI-N87 cells are more desirable than SNU-216 for proving the concept of this study.

In overall, this study might be able to support the fact that ultrasound- mediated delivery of microbubbles can be a convincing and effective method for delivering therapeutic agents including chemotherapeutic drugs to enhance the cytotoxic effects.

Nevertheless, there are some limitations in this study in spite of these promising findings. First, this study was an *in vitro* experiment. The exact delivery effect of cisplatin by ultrasound-guided microbubbles *in vivo* may not be extrapolated from this study. Thus, further *in vivo* studies evaluating the effects of MLCs are warranted to expand our result to clinical applications. Second, we did not perform flow cytometry in the assessment of cellular targeting by MLCs, which may have

allowed more accurate quantitative evaluation than with confocal microscopic examination alone. Third, as shown by the comparison results for NCI-N87 cells between the four experimental groups at 75 hours, the cytotoxic effect was significant when cisplatin was added to the MLCs. On the other hand, the evidence of weak to prove the additional therapeutic effect of US-flashing, which could have been anticipated by the specific features of ultrasound such as sonoporation. The therapeutic effect observed in this study seems to owe more to the specific targeting effect of the antibody-conjugated MLC, rather than to the effect of ultrasound.

In conclusion, MLC could effectively target gastric cancer cell lines by conjugating anti-HER2 antibody followed by ultrasound exposure. It could effectively deliver cisplatin into target cells under ultrasound, resulting in significant decrease in cancer cell viability rates. Therefore, this study may provide promising methods for delivering chemotherapeutic drugs to gastric cancer cells. We envision that this technique could promote clinical applications of targeted therapy in the future.

REFERENCES

1. Ferlay J SI, Ervik M, Dikshit R, Eser S, Mathers C, Rebelo M, Parkin DM, Forman D, Bray, F. GLOBOCAN 2012 v1.0, Cancer Incidence and Mortality Worldwide: IARC CancerBase No. 11 [Internet]. Lyon, France: International Agency for Research on Cancer; 2013 [cited 2015 17/07]. Available from: http://globocan.iarc.fr, accessed on 17/07/2015.

2. Jung KW, Won YJ, Kong HJ, Oh CM, Cho H, Lee DH, et al. Cancer statistics in Korea: incidence, mortality, survival, and prevalence in 2012. Cancer research and treatment : official journal of Korean Cancer Association. 2015;47(2):127-41.

3. Buzzoni R, Bajetta E, Di Bartolomeo M, Miceli R, Beretta E, Ferrario E, et al. Pathological features as predictors of recurrence after radical resection of gastric cancer. The British journal of surgery. 2006;93(2):205-9.

4. Field K, Michael M, Leong T. Locally advanced and metastatic gastric cancer: current management and new treatment developments. Drugs. 2008;68(3):299-317.

5. Wagner AD, Unverzagt S, Grothe W, Kleber G, Grothey A, Haerting J, et al. Chemotherapy for advanced gastric cancer. The Cochrane database of systematic reviews. 2010(3):CD004064.

6. De Vita F, Giuliani F, Silvestris N, Catalano G, Ciardiello F, Orditura M. Human epidermal growth factor receptor 2 (HER2) in gastric cancer: a new therapeutic target. Cancer treatment reviews. 2010;36 Suppl 3:S11-5.

7. Grabsch H, Sivakumar S, Gray S, Gabbert HE, Muller W. HER2 expression in gastric cancer: Rare, heterogeneous and of no prognostic value - conclusions from 924 cases of two independent series. Cellular oncology : the official journal of the International Society for Cellular Oncology. 2010;32(1-2):57-65.

8. Nakajima M, Sawada H, Yamada Y, Watanabe A, Tatsumi M, Yamashita J, et al. The prognostic significance of amplification and overexpression of c-met and c-erb B-2 in human gastric carcinomas. Cancer. 1999;85(9):1894-902.

9. Orita H, Maehara Y, Emi Y, Kakeji Y, Baba H, Korenaga D, et al. c-erbB-2 expression is predictive for lymphatic spread of clinical gastric carcinoma.

Hepato-gastroenterology. 1997;44(13):294-8.

10. Seock Ah Im KEL, Eunmi Nam, Seung Hyun Nam, Do Yeun Kim, Chu Myong Seong, Hae Young Park, Woon Sup Han, Ju Young Seoh, Soon Nam Lee. The Prognostic Significance of the Overexpression of HER-2/ neu in Korean Gastric Carcinomas and the In Vitro Effects of Anti-HER-2/neu Antibody on Cell Growth in the Gastric Carcinoma Cell Lines. Cancer research and treatment : official journal of Korean Cancer Association. 2003;35(2):109-16.

11. Bang YJ, Van Cutsem E, Feyereislova A, Chung HC, Shen L, Sawaki A, et al. Trastuzumab in combination with chemotherapy versus chemotherapy alone for treatment of HER2-positive advanced gastric or gastro-oesophageal junction cancer (ToGA): a phase 3, open-label, randomised controlled trial. Lancet. 2010;376(9742):687-97.

12. Nomikou N, McHale AP. Exploiting ultrasound-mediated effects in delivering targeted, site-specific cancer therapy. Cancer letters. 2010;296(2):133-43.

13. Pochon S, Tardy I, Bussat P, Bettinger T, Brochot J, von Wronski M, et al.

BR55: a lipopeptide-based VEGFR2-targeted ultrasound contrast agent for molecular imaging of angiogenesis. Investigative radiology. 2010;45(2):89-95.

14. Pysz MA, Foygel K, Rosenberg J, Gambhir SS, Schneider M, Willmann JK. Antiangiogenic cancer therapy: monitoring with molecular US and a clinically translatable contrast agent (BR55). Radiology. 2010;256(2):519-27.

15. Pysz MA, Machtaler SB, Seeley ES, Lee JJ, Brentnall TA, Rosenberg J, et al. Vascular endothelial growth factor receptor type 2-targeted contrast-enhanced US of pancreatic cancer neovasculature in a genetically engineered mouse model: potential for earlier detection. Radiology. 2015;274(3):790-9.

16. Bachawal SV, Jensen KC, Wilson KE, Tian L, Lutz AM, Willmann JK. Breast Cancer Detection by B7-H3-Targeted Ultrasound Molecular Imaging. Cancer research. 2015;75(12):2501-9.

17. Yoon YI, Kwon YS, Cho HS, Heo SH, Park KS, Park SG, et al. Ultrasound-mediated gene and drug delivery using a microbubble-liposome particle system. Theranostics. 2014;4(11):1133-44.

18. Wang TY CJ, Pu K, Devulapally R, Bachawal S, Machtaler S, Chowdhury SM, Luong R, Tian L, Khuri-Yakub B, Rao 1, Paulmurugan R, Willmann JK. Ultrasound-guided delivery of microRNA loaded nanoparticles into cancer. Journal of controlled release : official journal of the Controlled Release Society. 2015;10(203):99-108.

19. Ku JL, Park JG. Biology of SNU cell lines. Cancer research and treatment : official journal of Korean Cancer Association. 2005;37(1):1-19.

20. Kim MA, Lee HS, Lee HE, Jeon YK, Yang HK, Kim WH. EGFR in gastric carcinomas: prognostic significance of protein overexpression and high gene copy number. Histopathology. 2008;52(6):738-46.

21. Fujimoto-Ouchi K, Sekiguchi F, Yasuno H, Moriya Y, Mori K, Tanaka Y. Antitumor activity of trastuzumab in combination with chemotherapy in human gastric cancer xenograft models. Cancer chemotherapy and pharmacology. 2007;59(6):795-805.

22. Ishiyama M, Tominaga H, Shiga M, Sasamoto K, Ohkura Y, Ueno K. A

combined assay of cell viability and in vitro cytotoxicity with a highly water-soluble tetrazolium salt, neutral red and crystal violet. Biological & pharmaceutical bulletin. 1996;19(11):1518-20.

23. Wang X, Liang HD, Dong B, Lu QL, Blomley MJ. Gene transfer with microbubble ultrasound and plasmid DNA into skeletal muscle of mice: comparison between commercially available microbubble contrast agents. Radiology. 2005;237(1):224-9.

24. Hernot S, Klibanov AL. Microbubbles in ultrasound-triggered drug and gene delivery. Advanced drug delivery reviews. 2008;60(10):1153-66.

25. Liu Y, Ling Y, Qi Q, Zhu M, Wan M, Zhang Y, et al. Trastuzumab increases the sensitivity of HER2-amplified human gastric cancer cells to oxaliplatin and cisplatin by affecting the expression of telomere-associated proteins. Oncology letters. 2015;9(2):999-1005.

26. Kim SY, Kim HP, Kim YJ, Oh do Y, Im SA, Lee D, et al. Trastuzumab inhibits the growth of human gastric cancer cell lines with HER2

amplification synergistically with cisplatin. International journal of oncology. 2008;32(1):89-95.

국문 초록

서론: 위암은 암 사망의 가장 흔한 원인 중 하나이다. HER-2는 진행성위암의 치료에 정립된 분자적 표적물질이다. 본 연구는 항암제를 HER2-양성 위암에 효과적으로 전달하기 위해 trastuzumab을 탑재한 표적 초음파 조영제를 합성하고 HER2-양성 위암세포주를 대상으로 한 시험관내 효과 분석을 하고자 한다.

방법: 동물실험은 동물실험윤리위원회의 승인을 받았다. 인간위암세포주 NCI-N87, SNU-216, SNU-484, 그리고 SNU-601을 배양하였다. HER2를 표적으로 하는 초음파 조영제를 만들기 위해 지질막과 육플루오르화황 가스 중심부를 갖는 미세기포지질복합체(MLC)를 합성하였다. 미세기포지질복합체에 HER2-항체 (trastuzumab, Herceptin®)를 결합시켜 HER2-양성 위암세포를 표적으로 삼을 수 있게 하였다. MLC-$HER2_{Ab}$에 형광물질을 첨가하여 위암세포들과 함께 배양한 뒤, 공초점 레이저 주사 현미경으로 표적 세포에의 결합 여부를 평가하였다. 이후 MLC-$HER2_{Ab}$에 cisplatin을 추가하여 NCI-N87 및 SNU-484 위암세포들과 함께 배양하여 세포 독성 치료 효과를 평가하였다. 이 때 초음파에 추가적으로 노출시켜 초음파-경유 복합체의 전달효과도 탐색하였다.

결과: 공초점 레이저 주사 현미경 상, HER2-양성 위암세포주인 NCI-N87과 SNU-216에서 선택적인 MLC-$HER2_{Ab}$의 결합을 관찰하였다. NCI-N87 세포들에서 cisplatin을 탑재한 MLC-$HER2_{Ab}$ 과 초음파를 처리하였을 때 증가된 세포 독성을 확인하였으나, SNU-484 세포들에서는 이러한 효과를 관찰하지 못하였다.

결론: 미세기포지질복합체에 trastuzumab을 결합시켜 HER2-양성 위암세포주에

선택적으로 전달할 수 있었다. 이는 초음파 처리 하에 cisplatin을 표적 세포들에 보다 효과적으로 전달하여 세포독성을 일으켰다. 따라서 MLC는 초음파-경유 표적 치료제의 전달에 유망한 방법이 될 수 있다.

주요어: 초음파, 미세기포, 표적치료, 위암
학번 : 2013 – 30827